

EFFECT OF SHEAR FLEXIBILITY IN BUCKLING ANALYSIS OF BEAM STRUCTURES

Asoc. Prof. Lanc D. PhD.¹, Prof. Turkalj G. PhD.¹, Asist. Pešić I. PhD.¹
Faculty of Engineering, University of Rijeka, Croatia ¹

dlanc@riteh.hr

Abstract: Paper deals with finite element buckling analysis of shear deformable beam-type structures. Displacements and rotations are allowed to be large but strains are assumed to be small. The corresponding equilibrium equations are formulated in the framework of co-rotational description, using the virtual work principle. Displacements and rotations are allowed to be large while strains are assumed to be small. Linear shape functions are used for the axial displacement, while cubic shape functions are employed for transverse displacements and angle of twist. The algorithm is validated on test examples.

Keywords: FINITE ELEMENT, SHEAR FLEXIBILITY, BUCKLING, BEAM, STABILITY

1. Introduction

Load-carrying structures composed of thin-walled sections are extensively used in engineering practice, both in stand-alone forms and as stiffeners for plate-like or shell-like structures. Unfortunately, such weight-optimised structural components, especially those with open profiles, are commonly weak in torsion and very susceptible to instability or buckling failure [1, 2].

Results of classical Euler-Bernoulli theory for bending and torsion of thin-walled beams do not always agree with experimental results and that is mainly caused by neglecting the shear deformations in cross sectional plane as results of transversal forces and restricted warping [1]. Shear-flexible beam finite element developed in this paper takes into account shear deformation effects during the bending and torsion.

This work presents a one-dimensional shear flexible finite element formulation for non-linear analysis of beam structures. Beam members are supposed to be straight and prismatic. Spatial displacements and rotations are allowed to be large but strains are assumed to be small. Using virtual work principle and assuming isotropic and linear-elastic material a tangent stiffness matrix of a two-node space beam element is developed in local Eulerian coordinate system. This system follows the element chord during deformation so this approach is linear in local system.

Numerical results are obtained for cantilever as well as simply-supported beam. Beam high to span ratios influence on the critical buckling loads are also considered. Numerical results show that the shear effects play very important role on the buckling analysis of beams.

2. Basic consideration

Cross sectional displacements are defined with rigid-body translational components w_0, u_0, v_0 , rigid-body rotational components $\varphi_x, \varphi_y, \varphi_z$ and θ component defining warping of cross-section.

In used right handed Cartesian coordinate system (z, x, y) , axis z coincident with beam axis passing through the centroids O of cross sections. Coordinate axes x and y are cross sectional principal axes of inertia. Cross sectional points are defined with x and y coordinates and warping function $\omega = \omega(x, y)$.

Assuming that displacement and rotations are small in local Eulerian coordinate system follows the displacement field:

$$\begin{aligned} w(z, x, y) &= w_0(z) - y \varphi_x(z) - x \varphi_y(z) - \omega(x, y) \theta(z) \\ u(z, x, y) &= u_0(z) - y \varphi_z(z) \\ v(z, x, y) &= v_0(z) + x \varphi_z(z) \end{aligned} \quad (1)$$

Strain tensor can be written as:

$$e_{ij} = 0.5(u_{i,j} + u_{j,i}) \quad (2)$$

The stress resultant of cross section consist of following components [3]: axial force F_z ; shearforces F_x, F_y ; bending moments M_x, M_y ; torsional moment M_z ; bimoment M_ω .

$$\begin{aligned} F_z &= \int_A \sigma_z dA, \quad F_x = \int_A \tau_{zx} dA, \quad F_y = \int_A \tau_{zy} dA, \quad M_x = \int_A \sigma_z y dA, \\ M_y &= -\int_A \sigma_z x dA, \quad M_z = \int_A [\tau_{zy} x - \tau_{zx} y] dA = T_{sv} + T_\omega, \quad M_\omega = \int_A \sigma_z \omega dA. \end{aligned}$$

In equation for torsional moment T_{sv} represents St.Venant or uniform torsional moment while T_ω is the warping or non-uniform torsional moment.

Considering the shear deformation due to F_x, F_y and T_ω we have:

$$\begin{aligned} \varphi_x \neq -\frac{dv_s}{dz} &\Rightarrow \frac{dv_s}{dz} + \varphi_x = \bar{\gamma}_{zy}, \quad \varphi_y \neq -\frac{du_s}{dz} \Rightarrow \frac{du_s}{dz} - \varphi_y = \bar{\gamma}_{zx}, \\ \theta \neq -\frac{d\varphi_z}{dz} &\Rightarrow \frac{d\varphi_z}{dz} + \theta = \bar{\gamma}_\omega \end{aligned} \quad (3)$$

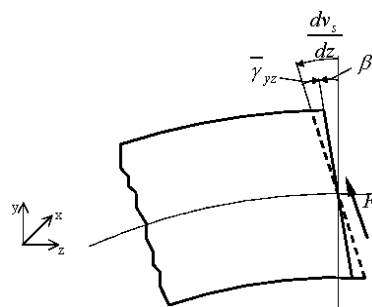


Fig. 1 Shear deformation in y-z plane.

In the plane y-z, according to (Fig. 1), we have:

$$\begin{aligned} \frac{dv_s}{dz} - \beta_x &= \frac{dv_s}{dz} + \varphi_x = \bar{\gamma}_{zy} \\ M_x &= -EI_x \frac{d\beta_x}{dz} = EI_x \frac{d\varphi_x}{dz} \\ F_y &= \bar{\tau}_{zy} \cdot A_y = G \cdot \bar{\gamma}_{zy} \cdot A_y = \frac{GA}{k_y} \left(\varphi_x + \frac{dv_s}{dz} \right) \end{aligned} \quad (4)$$

and the same, for bending in x-y plane follows:

$$\begin{aligned} \frac{du_x}{dz} - \beta_y &= \frac{du_x}{dz} - \varphi_y = \bar{\gamma}_{xz} \\ M_y &= EI_y \frac{d\beta_y}{dz} = EI_y \frac{d\varphi_y}{dz} \\ F_x &= \bar{\tau}_{xz} \cdot A_x = G \cdot \bar{\gamma}_{xz} \cdot A_x = \frac{GA}{k_x} \left(\frac{du_x}{dz} - \varphi_y \right) \end{aligned} \quad (5)$$

in equations above $\bar{\gamma}_{xz}, \bar{\gamma}_{zy}$ are average values of shear deformations, $\bar{\tau}_{xz}, \bar{\tau}_{zy}$ are average values of shear stresses, A_x, A_y are shear areas and k_x, k_y are flexible shear coefficients.

On an analogous way for torsion follows:

$$\begin{aligned} \frac{d\varphi_z}{dz} + \theta &= \bar{\gamma}_\omega \\ M_\omega &= EI_\omega \frac{d\theta}{dz}; \quad T_{SV} = GJ \frac{d\varphi_z}{dz} \\ T_\omega &= G\bar{\gamma}_\omega J_\omega = \frac{GJ}{k_\omega} \left(\frac{d\varphi_z}{dz} + \theta \right) \end{aligned} \quad (6)$$

where J_ω is shear area with respect to ω and k_ω is shear factor due to restricted warping.

3. Finite element formulation

The nodal displacement vector of the e-th beam finite element from (Fig. 2) is:

$$\left(\mathbf{u}^e \right)^T = \left\{ w_B, \varphi_{zB}, \varphi_{xA}, \varphi_{xB}, \varphi_{yA}, \varphi_{yB}, \theta_A, \theta_B \right\} \quad (7)$$

and appropriate nodal force vector is:

$$\left(\mathbf{f}^e \right)^T = \left\{ F_{zB}, M_{zB}, M_{xA}, M_{xB}, M_{yA}, M_{yB}, M_{\omega A}, M_{\omega B} \right\} \quad (8)$$

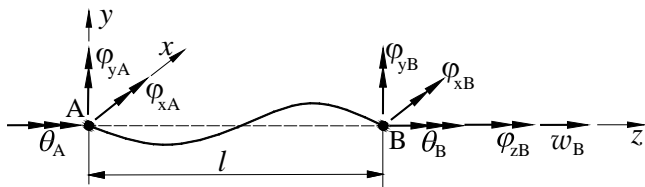


Fig. 2 Two-nodded beam element.

According to the principle of virtual work [4] it is:

$$\delta U_E - \delta W = \delta \Pi = 0 \quad (9)$$

where $\delta U_E = \int_V S_{ij} \delta e_{ij} dV$ is the elastic potential energy of internal forces, $\delta W = \int_{A_\sigma} t_i \delta u_i dA_\sigma$ is the virtual work of external forces, Π is the total potential energy, S_{ij} is the stress tensor, δe_{ij} is the strain tensor, t_i are surface forces and u_i are displacement components.

Substituting Equations (2)-(8) into the relations for δU_E follows:

$$\begin{aligned} \delta U_E = \int_0^l \left[EA \frac{dw_\omega}{dz} \delta \frac{dw_\omega}{dz} + EI_x \frac{d\varphi_x}{dz} \delta \frac{d\varphi_x}{dz} + EI_y \frac{d\varphi_y}{dz} \delta \frac{d\varphi_y}{dz} + EI_\omega \frac{d\theta}{dz} \delta \frac{d\theta}{dz} + \right. \\ \left. + GJ \frac{d\varphi_z}{dz} \delta \frac{d\varphi_z}{dz} + \frac{GA}{k_x} \left(\frac{dv_x}{dz} - \varphi_x \right)^2 + \frac{GA}{k_y} \left(\frac{du_x}{dz} + \varphi_y \right)^2 + \frac{GJ}{k_\omega} \left(\frac{d\varphi_z}{dz} + \theta \right)^2 \right] dz \quad (10) \end{aligned}$$

Considering for finite element in y-z plane:

$$F_y = \frac{dM_x}{dz}, \quad M_x = EI_x \frac{d\varphi_x}{dz}, \quad F_y = \frac{GA}{k_y} \left(\frac{dv_x}{dz} - \varphi_x \right), \quad \frac{dF_y}{dz} = 0$$

With: $z=0 \rightarrow \varphi_x = \varphi_{xA}, \quad z=l \rightarrow \varphi_x = \varphi_{xB}$ and substitution $\xi = z/l$, follows:

$$v_\omega = \mathbf{N}_v \mathbf{v}, \quad \varphi_x = \mathbf{N}_{\varphi_x} \mathbf{v}, \quad \mathbf{v}^T = \left\{ \varphi_{xA} \quad \varphi_{xB} \right\}, \quad (11)$$

where \mathbf{N}_v and \mathbf{N}_{φ_x} are matrices of interpolation functions:

$$\begin{aligned} \mathbf{N}_v &= \left[\frac{-l(\xi^3 - 2(1+3\Psi_y)\xi^2 + (1+6\Psi_y)\xi)}{\Omega_y}; \frac{-l(\xi^3 - (1-6\Psi_y)\xi^2 - 6\Psi_y\xi)}{\Omega_y} \right] \\ \mathbf{N}_{\varphi_x} &= \left[\frac{3\xi^3 - 4(1+3\Psi_y)\xi + \Omega_y}{\Omega_y}; \frac{3\xi^2 - 2(1-6\Psi_y)\xi}{\Omega_y} \right] \end{aligned}$$

Analogously for bending in x-z plane the interpolations are:

$$\begin{aligned} \mathbf{N}_u &= \left[\frac{l(\xi^3 - 2(1+3\Psi_x)\xi^2 + (1+6\Psi_x)\xi)}{\Omega_x}; \frac{l(\xi^3 - (1-6\Psi_x)\xi^2 - 6\Psi_x\xi)}{\Omega_x} \right] \\ \mathbf{N}_{\varphi_y} &= \left[\frac{3\xi^3 - 4(1+3\Psi_x)\xi + \Omega_x}{\Omega_x}; \frac{3\xi^2 - 2(1-6\Psi_x)\xi}{\Omega_x} \right] \end{aligned}$$

and for torsion :

$$\begin{aligned} \mathbf{N}_{\varphi_z} &= \left[\frac{-2\xi^3 + 3\xi^2 + 12\Psi_\omega\xi}{\Omega_\omega}; \frac{-l(\xi^3 - 2(1+3\Psi_\omega)\xi^2 + (1+6\Psi_\omega)\xi)}{\Omega_\omega}; \right. \\ &\quad \left. \frac{-l(\xi^3 - (1-6\Psi_\omega)\xi^2 - 6\Psi_\omega\xi)}{\Omega_\omega} \right] \\ \mathbf{N}_\theta &= \left[\frac{6\xi^2 - 6\xi}{l \cdot \Omega_\omega}; \frac{3\xi^3 - 4(1+3\Psi_\omega)\xi + \Omega_\omega}{\Omega_\omega}; \frac{3\xi^2 - 2(1-6\Psi_\omega)\xi}{\Omega_\omega} \right] \end{aligned}$$

so displacements are:

$$u_\omega = \mathbf{N}_u \mathbf{u}, \quad \varphi_y = \mathbf{N}_{\varphi_y} \mathbf{u}, \quad \mathbf{u}^T = \left\{ \varphi_{yA} \quad \varphi_{yB} \right\} \quad (12)$$

$$\varphi_z = \mathbf{N}_{\varphi_z} \boldsymbol{\varphi}, \quad \theta = \mathbf{N}_\theta \boldsymbol{\varphi}, \quad \boldsymbol{\varphi}^T = \left\{ \varphi_{zB} \quad \theta_A \quad \theta_B \right\} \quad (13)$$

For axial displacement linear interpolation function is used:

$$w_\omega = \mathbf{N}_w \mathbf{w}, \quad \mathbf{w}^T = \left\{ w_B \right\}, \quad \mathbf{N}_w = \left[\xi \right]. \quad (14)$$

Finite element stiffness matrix results from integral (10) in form of 8x8 with non-zero components:

$$\begin{aligned} k_{1,1} &= \frac{AE}{l}; \quad k_{2,2} = \frac{12EI_\omega}{l^3\Omega_\omega} + \frac{6GJ(1+20\Psi_\omega+120\Psi_\omega^2)}{5l\Omega_\omega^2}; \\ k_{2,7} &= \frac{6EI_\omega}{l^2\Omega_\omega} + \frac{GJ}{10\Omega_\omega^2} = k_{7,2} = k_{2,8} = k_{8,2}; \\ k_{3,4} &= \frac{2(1-6\Psi_y)EI_x}{l\Omega_y} = k_{4,3}; \quad k_{5,5} = \frac{4(1+3\Psi_x)EI_y}{l\Omega_x} = k_{6,6}; \\ k_{5,6} &= \frac{2(1-6\Psi_x)EI_y}{l\Omega_x} = k_{6,5}; \quad k_{3,3} = \frac{4(1+3\Psi_y)EI_x}{l\Omega_y} = k_{4,4}; \\ k_{7,7} &= \frac{4(1+3\Psi_\omega)EI_\omega}{l\Omega_\omega} + \frac{2GJ(1+15\Psi_\omega+90\Psi_\omega^2)}{15\Omega_\omega^2} = k_{8,8}; \\ k_{7,8} &= \frac{2(1-6\Psi_\omega)EI_\omega}{l\Omega_\omega} - \frac{GJ(1+60\Psi_\omega+360\Psi_\omega^2)}{30\Omega_\omega^2} = k_{8,7} \end{aligned}$$

with:

$$\begin{aligned} \Omega_x &= 1+12\Psi_x; \quad \Psi_x = \frac{k_x I_y}{GA l^2}; \quad \Omega_y = 1+12\Psi_y; \quad \Psi_y = \frac{k_y I_x}{GA l^2}; \\ \Omega_\omega &= 1+12\Psi_\omega; \quad \Psi_\omega = \frac{k_\omega I_\omega}{GJ l^2} \end{aligned}$$

Element force vector transformed from local to global coordinate system is:

$$\bar{\mathbf{f}}^e = \mathbf{t}_1^e \mathbf{f}^e \tag{15}$$

The element global stiffness matrix $\bar{\mathbf{k}}$ can be obtained as follows:

$$\bar{\mathbf{k}} = (\mathbf{t}_1^e)^T \mathbf{k} \mathbf{t}_1^e + \mathbf{t}_2^e \mathbf{f}^e \tag{16}$$

$$\bar{k}_{i,j} = \sum_{k=1}^8 \left[\left(\sum_{m=1}^8 \mathbf{t}_{1,i,k}^e \cdot k_{k,m} \cdot \mathbf{t}_{1,j,m}^e \right) + \mathbf{t}_{2,i,j,k}^e \cdot \mathbf{f}^e_k \right] \tag{17}$$

In equations above \mathbf{t}_1^e is 14x8 transformation matrix that contains first derivations while \mathbf{t}_2^e is 14x14x8 matrix of second derivations of the local with respect to global displacements. Matrix \mathbf{t}_2^e presents geometric stiffness contribution because it contains effects on global forces caused with change in geometry. Evaluations of matrices \mathbf{t}_1^e and \mathbf{t}_2^e are explained in [5, 6].

Performing the standard assembly procedure, the overall incremental equilibrium equations can be obtained as:

$$\mathbf{K}_T \mathbf{U} = \mathbf{P} ; \mathbf{K}_T = \sum_e \bar{\mathbf{k}}_T^e, \quad \mathbf{P} = \sum_e \bar{\mathbf{f}}^e \tag{18}$$

where \mathbf{K}_T represent the tangential stiffness matrix of a structure, obtained from their counterparts on the element level, while \mathbf{U} and \mathbf{P} are the incremental displacement vector and the incremental external loads of the structure, respectively.

4. Examples

A first example presents a simple supported I-cross section beam. The lengths of beam varieties to be $L = 100; 200; 400; 800$ cm. The beam is loaded axially by the compression force F as it is shown on (Fig. 3).

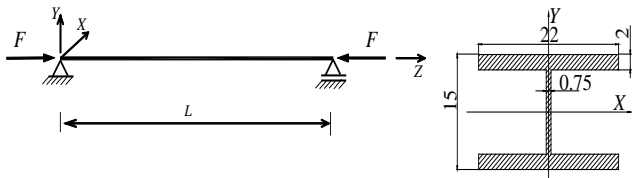


Fig. 3 Axially compressed simple beam.

Material moduli are: $E = 2,1 \cdot 10^7 \text{ Ncm}^{-2}$ and $G = 80,77 \cdot 10^5 \text{ Ncm}^{-2}$. Cross sectional properties are: moments of inertia $I_x = 3830,52 \text{ cm}^4$, $I_y = 3549,72 \text{ cm}^4$ and the cross sectional area $A = 96,25 \text{ cm}^2$, $k_x = 11,67$, $k_y = 1,3125$. To initiate buckling, a small lateral perturbation force $\Delta F = 10^{-5} F$ is performed at the mid-span point of beam in X-direction. Timoshenko [7, 8] analytical results are given in Tab.1.

Table 1: Critical buckling loads according to Timoshenko analytical formula

L [cm]	$F_{cr} \cdot 10^6$ [N]		R
	$k_x = 0$	$k_x = 11,67$	
100	79,392	36,222	54%
200	19,848	15,291	23%
400	4,962	4,618	7%
800	1,241	1,218	2%

Load-deflection curves representing the applied force versus mid-span point lateral displacement in direction of perturbation force are given only for shear flexible case in (Fig. 4). From obtained results, the very good congruence with Timoshenko analytical results is evident. Also, in Tab. 1, the load difference between shear flexible and shear rigid case suggest that for relatively short beams this difference is significant while for slender beams this shear effects are almost negligible.

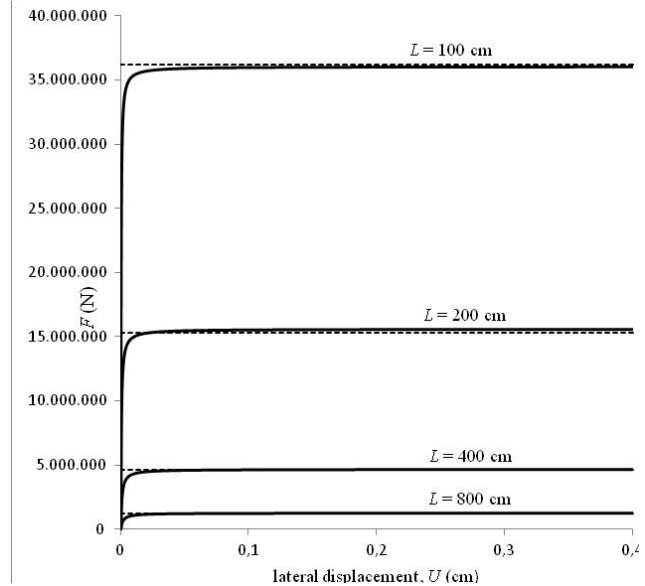


Fig. 4 Load displacement curves for beam length $l = 100; 200; 400; 800$ cm

The second example presents an axially loaded cantilever with doubly symmetric cross section, (Fig. 5). The lengths of cantilever is $L = 200$ cm while the material moduli are the same as in the previous example: $E = 2,1 \cdot 10^7 \text{ Ncm}^{-2}$ and $G = 80,77 \cdot 10^5 \text{ Ncm}^{-2}$. The cross sectional properties are: moments of inertia $I_x = I_y = 50 \text{ cm}^4$ and the cross sectional area $A = 20 \text{ cm}^2$, $k_x = k_y$. The perturbation force $\Delta F = 10^{-4} F$ is performed at point B in X-direction to initiate buckling. This example shows the influence of shear factor on critical buckling load.

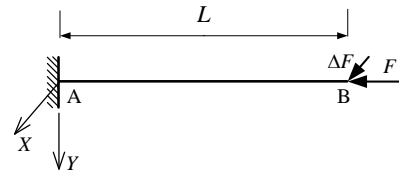


Fig. 5 Axially loaded cantilever.

On (Fig. 6), the load vs tip deflection curves for different values of shear factor $k_x = k_y = 0; 62,35; 124,70; 311,76; 623,52$. are given, as well as the Timoshenko analytical results for comparison.

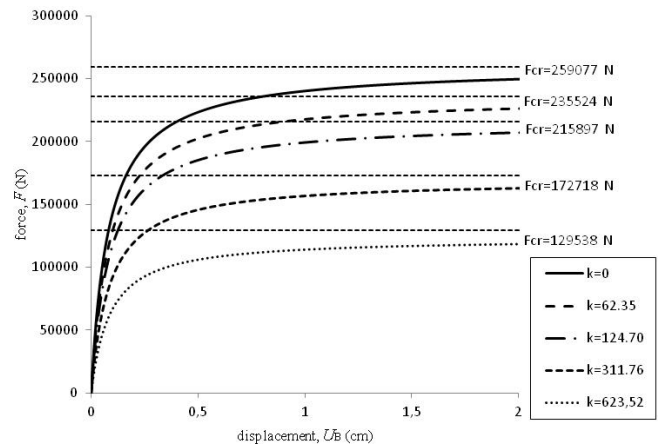


Fig. 6 Load vs displacement curves for cantilever for different values of shear factor k

4. Concluding remarks

Finite element numerical algorithm based shear flexible theory is developed. The present model is found to be appropriate and efficient in the field of the stability analysis of beam structures. Presented finite element includes both shear flexural deformation and torsional warping. Shear flexible deformations of cross section taken into account during analysis, guarantees results very precise

and close to theoretical values. Results of computer program comparing with analytic results, guaranties his successful applications.

5. Acknowledgement

The authors gratefully acknowledges financial support of Croatian Science Foundation (project No. 6876) and University of Rijeka (13.09.1.1.03 and 13.09.2.2.20).

6. References

- [1] G. Turkalj, D. Lanc and J. Brnić, "Stability Analysis of thin-walled frames using a shear-flexible beam element", in Topping, B.H.V. & Mota Soares C.A. (eds.), *Proceedings of the Seventh International Conference on Computational Structures Technology*, Civil-Comp Press, Stirling (Scotland), p.p. 569-570, 2004.
- [2] G. Turkalj, J. Brnić and J. Prpić Oršić, Large rotation analysis of elastic thin-walled beam-type structures using ESA approach, *Computers & Structures* **81**, p.p. 1851-1864, 2003.
- [3] G. Turkalj, J. Brnić and J. Prpić Oršić, ESA formulation for large displacement analysis of framed structures with elastic-plasticity, *Computers & Structures* **82**, p.p. 2001-2013, 2004.
- [4] Y.B. Yang, S.R. Kuo, *Theory & Analysis of Nonlinear Framed Structures*, Prentice Hall, New York, 1994.
- [5] G. Turkalj, J. Brnić and J. Prpić Oršić, Nonlinear stability analysis of thin-walled frames using UL-ESA formulation, *International Journal of Structural Stability and Dynamics* **4**, p.p. 45-67, 2004.
- [6] B.A.Izzuddin, An Eulerian approach to large displacement analysis of thinn-walled frames, *Proc. Instn Civ. Engrs Structs & Bldgs* **110**, p.p. 50-65, 1995.
- [7] B.A.Izzuddin, A.S. Elnashai, Eulerian formulation for large displacement analysis of space frames, *Journal of Engineering Mechanics* **119**, p.p. 549-569, 1993.
- [8] M.Y. Kim, S.P. Chang, S.B. Kim, "Spatial stability and free vibration of shear flexible thin-walled elastic beams. II: Numerical approach", *International Journal for Numerical Methods in Engineering*, 37, 4117-4140, 1994.
- [9] S.P. Timoshenko, J.M. Gere, *Theory of Elastic Stability*, Dover Publications inc., Mineola, New York, 2009.